Figure S1

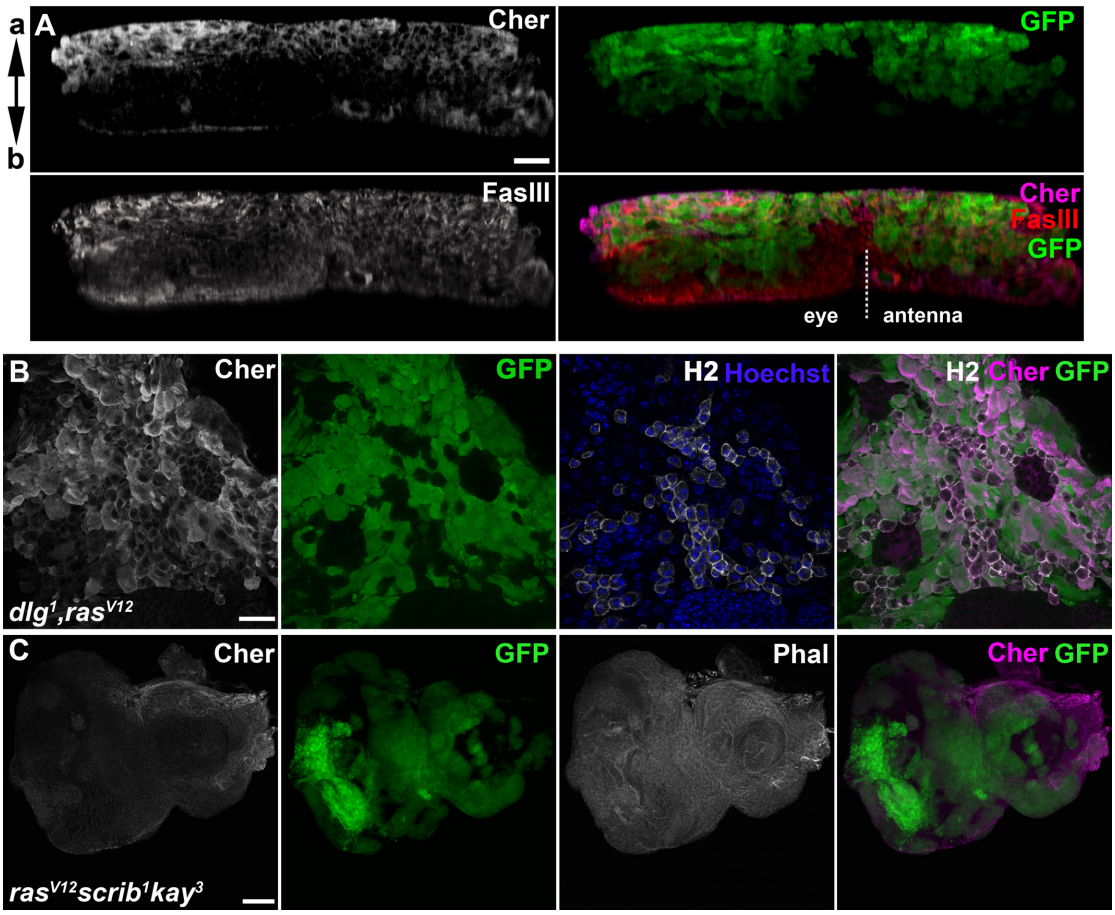

Figure S1. **Cher localizes to clonal tumors and EAD-associated hemocytes**.

(**A**) On day 7 AEL, Cher expression expands basally as *ras*^{V12}*scrib*^{1} PE clones overproliferate, generating multilayered masses. Disorganized pattern of Cher and FasIII staining indicates disturbed integrity of the PE and CE. (**B**) Cher protein accumulates in *ras*^{V12}*dlg*^{1} clonal tumors (7 days AEL) and associated hemocytes labeled by a pan-hemocyte H2 marker. (**C**) Absence of Fos function in *ras*^{V12}*scrib*^{1} clonal tumors by introducing a *kay*^{3} allele abolishes Cher up-regulation. (B) Cell nuclei were visualized using Hoechst staining. (A) Transversal sections of EAD with the apical side up; the dashed lines divide the eye and antennal parts of the EAD. Posterior is to the left. (B, C) are maximal projection of multiple confocal sections. Scale bars: 20 µm (A, B), 100 µm (C).

Figure S2

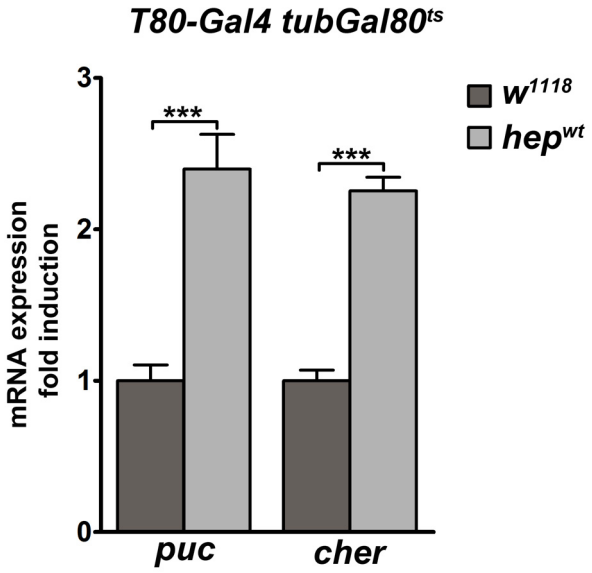

Figure S2. **JNK is sufficient to induce *cher* mRNA expression**. qRT-PCR shows up-regulation of *puckered* (*puc*) and *cher* transcripts upon temporary ubiquitous expression of wild-type JNK kinase Hemipterous (Hep^{wt}) in third-instar larvae using the heat-shock inducible TARGET system (McGuire et al., 2003). RNA was isolated from the whole larvae 6 h after a 60-min heat-shock at 37°C. Data are means ± s.e.m; $n = 5$; ***$p<0.001$.

Figure S3

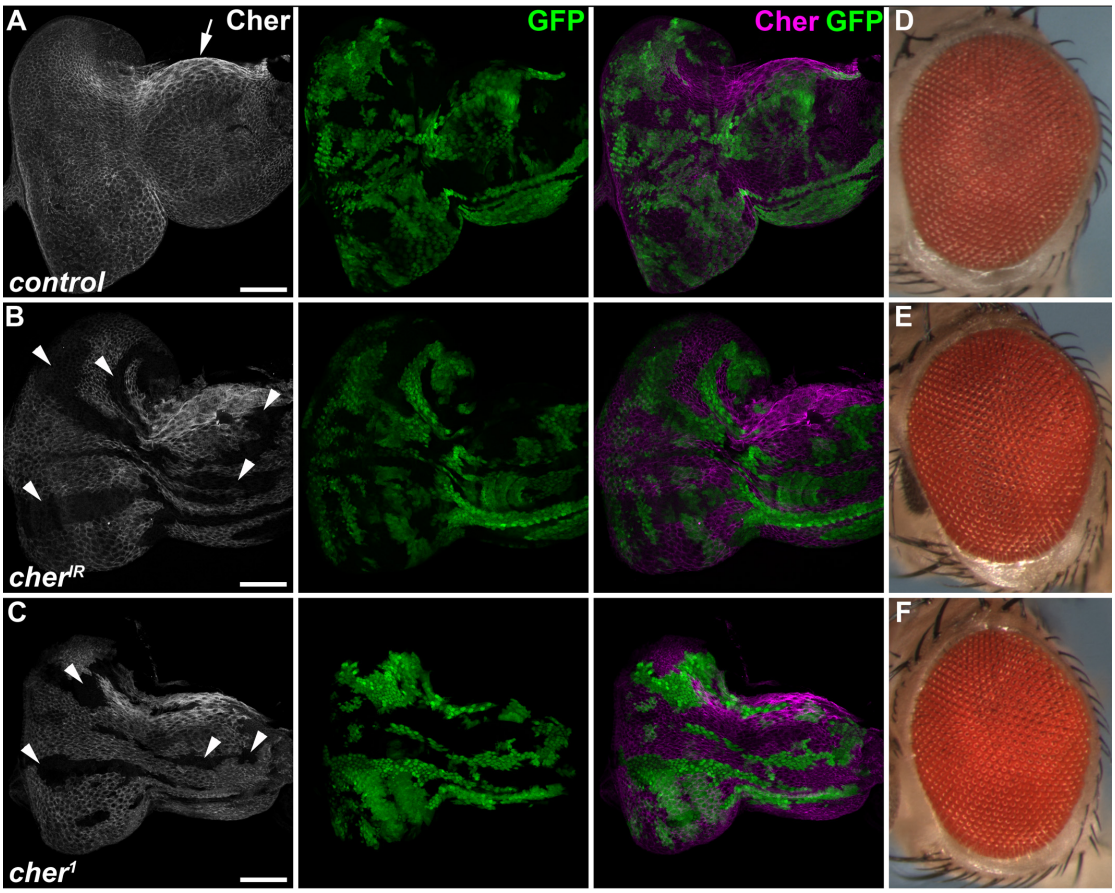

Figure S3. **Cher is dispensable for *Drosophila* eye development**. (**A-C**) Confocal projections show Cher staining of EAD carrying GFP labeled clones of the indicated genotypes 6 days AEL. (**A**) In control, Cher protein localizes apically to the cells of the PE with a slightly stronger staining in a stripe on the medial side of the antenna (arrow). (**B**) In clones expressing UAS-*cher*^{RNAi} transgene or (**C**) in *cher*^{1} homozygous null clones Cher staining vanishes (white arrowheads) compared to the non-clonal tissue, reflecting the efficiency of the RNAi knock-down and the loss of function allele, respectively. Scale bars: 50 µm. (D-F) Bright-field images of adult eyes carrying clones of the indicated genotypes. Neither *cher* RNAi (E) nor presence of homozygous mutant *cher*^{1} clones (F) affect the adult eye development.

Figure S4

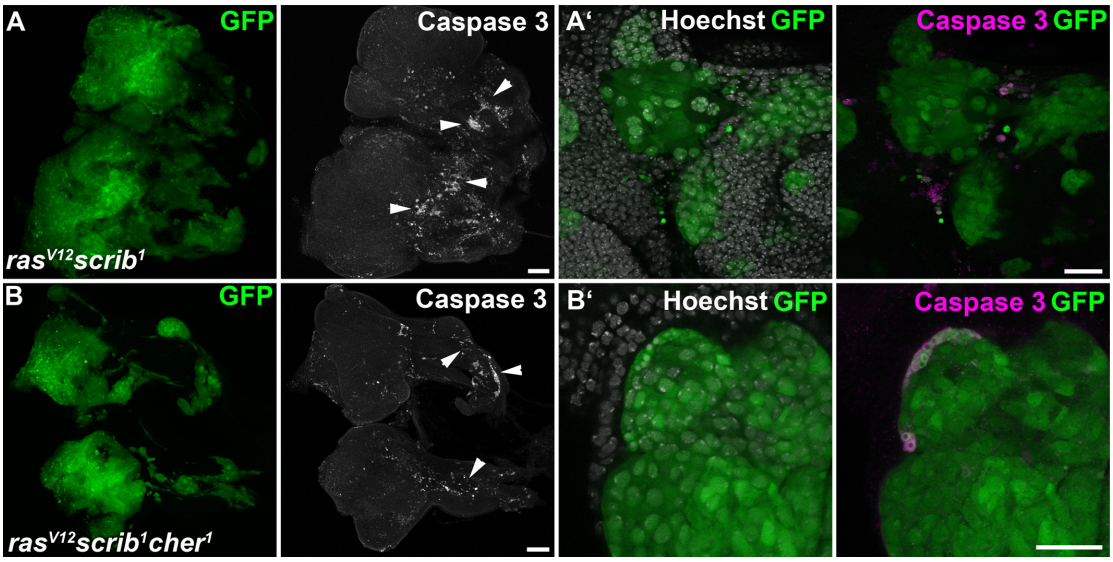

Figure S4. **Loss of *cher* does not compromise tumor cell viability.** (**A, B**) Caspase 3 positive cells accumulate mainly within the antenna parts of the mosaic EAD (white arrowheads) and clones (GFP^+) mutant for $ras^{V12}scrib^1$ (A) or $ras^{V12}scrib^1cher^1$ (**B**) show apoptosis at the clonal edges (A', B'). Yet number of Caspase 3 positive cells were similar in both genotypes as determined by FACS (Fig. 3D). Hoechst stains the nuclei. Images are projections of multiple confocal sections, scale bars are 50 µm (A, B) or individual sections of selected clonal areas, scale bars: 20 µm (A', B').

Figure S5

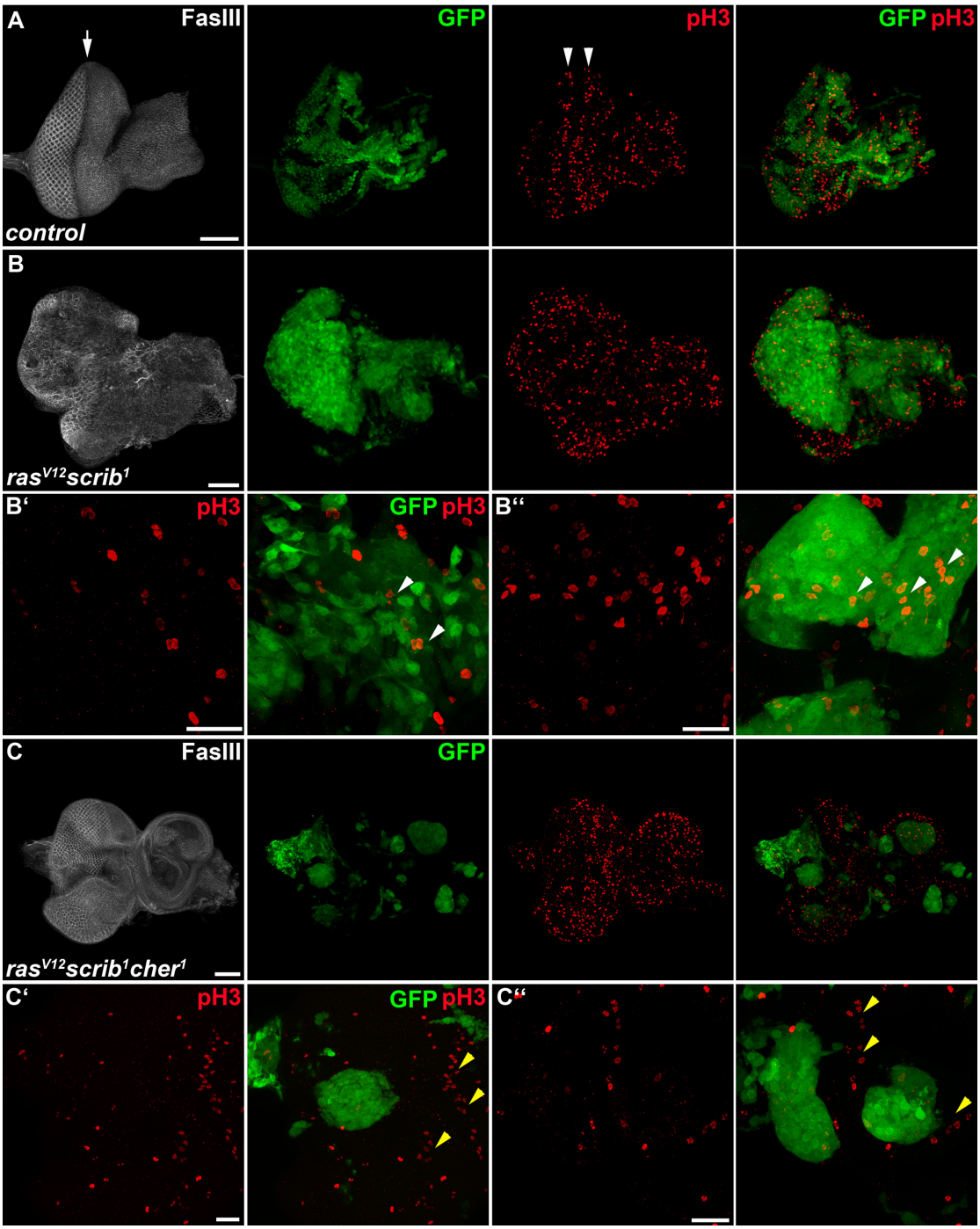

Figure S5. **Loss of Cher impedes tumor proliferation while promoting non-autonomous overgrowth.** (A-C) In control EAD (A), synchronous mitoses occur in two consecutive waves (marked by arrowheads) flanking the morphogenetic furrow, which is almost devoid of proliferating, pH3-positive cells. In $ras^{V12}scrib^{1}$ EAD (B), the mitotic waves and ommatidial structure become blurred with numerous cells

dividing in the posterior part of the disc. Clonal GFP^{+} (white arrowheads) as well as non-clonal cells label pH3-positive posterior (B') and anterior (B'') to the MF. In $ras^{V12}scrib^{1}cher^{1}$ EAD (C), non-clonal GFP-negative cells account for most of the proliferation (yellow arrowheads). Note that $ras^{V12}scrib^{1}cher^{1}$ clones (C) are round and smaller than $ras^{V12}scrib^{1}$ clones (B). Staining with FasIII reveals the boundary between region of differentiation, where clusters of ommatidia form, and undifferentiated cells localized anterior to the MF (arrow in A). Note the partly restored organization of ommatidia in $ras^{V12}scrib^{1}cher^{1}$ (C) compared to $ras^{V12}scrib^{1}$ clones (B). EAD were dissected 6 days AEL. Posterior is to the left. Panels (A-C) are projections through the entire EAD; scale bars: 50 µm. Panels (B', B'', C', C'') show individual sections of selected clonal areas; scale bars: 20 µm.

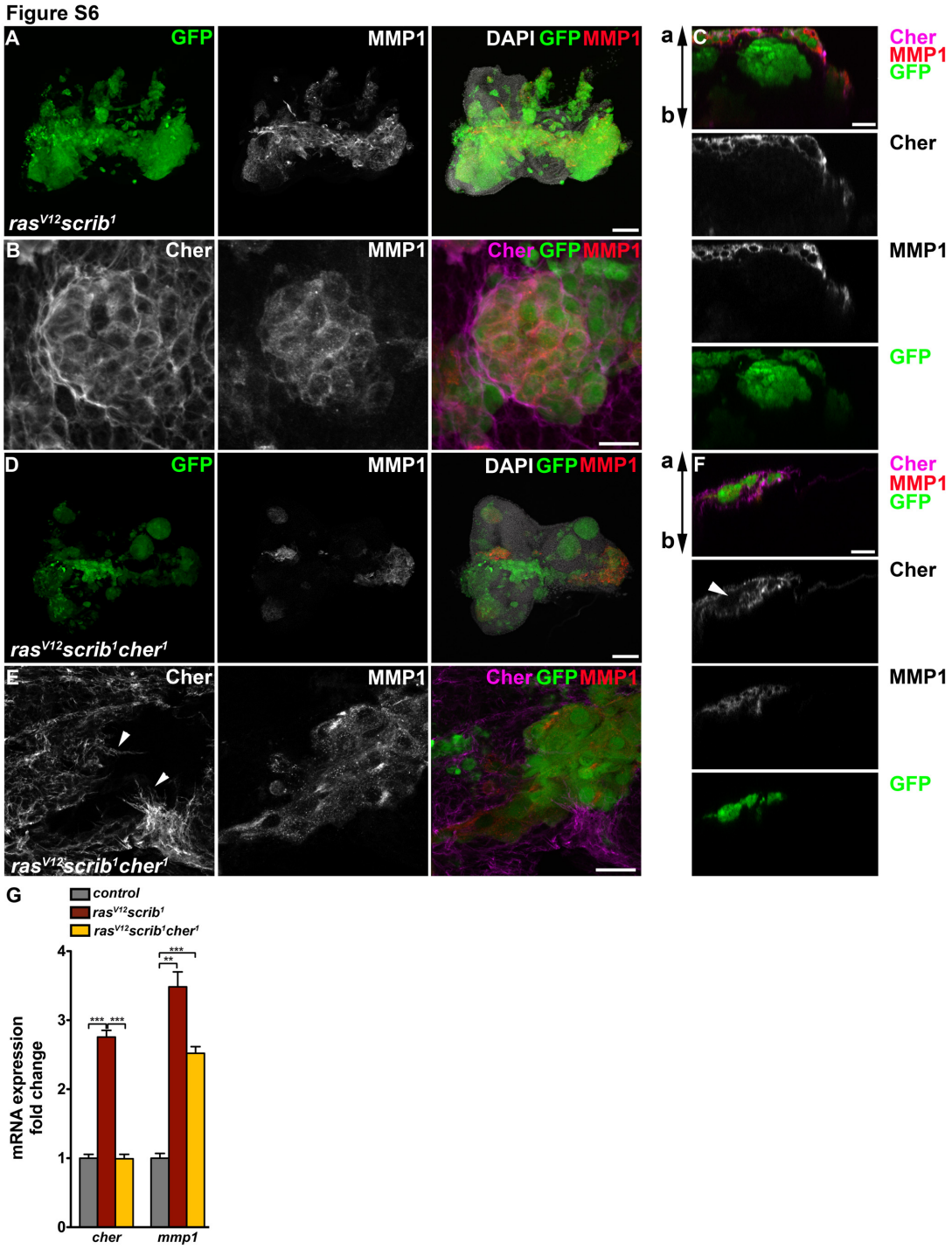

Figure S6. **Cher is not required for JNK-mediated MMP1 expression**. EAD carrying GFP-marked clones of the indicated genotypes (6 days AEL) were stained with Cher and MMP1 antibody. (A-C) MMP1 and Cher accumulate in EAD carrying *ras*^{V12}*scrib*^{1} tumors (A) and co-localize in the apical *ras*^{V12}*scrib*^{1} clones of the PE (B, C). (D-F) *ras*^{V12}*scrib*^{1}*cher*^{1} clones lack Cher while retaining enhanced MMP1 levels.

Mmp1 expression persist also in $ras^{V12}scrib^{1}cher^{1}$ clones confined between PE and CE (F). Note the Cher-labeled protrusions (white arrowheads) extended from non-clonal cells towards Cher-negative $ras^{V12}scrib^{1}$ clones. Panels show maximal projections of multiple confocal sections (A, D), single confocal sections (B, E) and transversal sections through the EAD with the apical side up (C, F). Scale bars: 50 μm (A, C, D, F) and 20 μm (B, E). (G) *mmp1* expression is significantly upregulated in $ras^{V12}scrib^{1}$ and $ras^{V12}scrib^{1}cher^{1}$ mosaic EAD (6 days AEL) relative to control. Expression of *cher* drops to control levels in EAD carrying $ras^{V12}scrib^{1}cher^{1}$ clones as determined by qRT-PCR. Data are means ± s.e.m; $n = 4$; $*p<0.05$, $**p<0.01$, and $***p<0.001$.

Figure S7

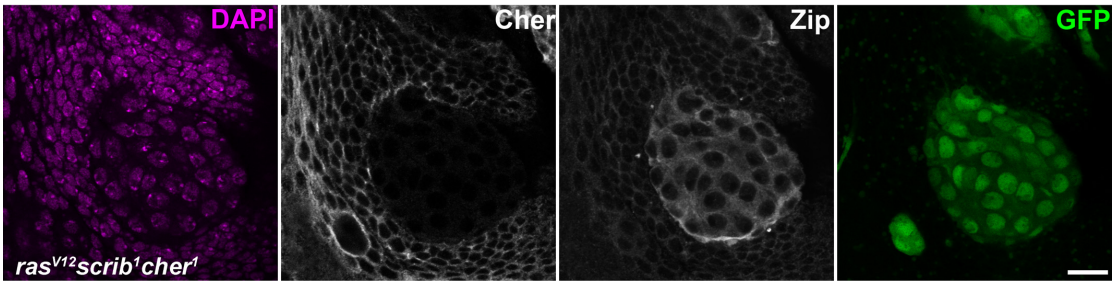

Figure S7. **Loss of Cher does not interfere with enrichment of Zip in clonal tumors**. Apical *ras*^{V12}*scrib*^{1}*cher*^{1} clones accumulate Zip protein relative to their non-clonal neighbors. Nuclei were counterstained with DAPI (magenta) EAD were dissected 7 days AEL. Panels show individual sections of selected clonal areas. Scale bar: 10 μm.

Supplemental Table S1

Primer Name	Sequence (5´- 3´)
Reporter Constructs	
SphI-cher-prom for	AAGCATGCGTAGTGTGGTTAGGAAAGTGAG
XhoI-cher-prom rev	TTCTCGAGCATTCGGATCCGCCATATCAG
cher-prom-ap1-A for	CGCGAAGGACTCCACAGAGCCAAAAAAAAAAAAAAAACCA GACAGACTACTCATCATATGTATG
cher-prom-ap1-B for	CATAGCTACCCGTTTTGACTTGTCAGAC TTTGGCTAAAATTAACAATTCCTAACCATATCG
cher-prom-ap1-C for	GGTGTGGGTGTGCAAGGGGATCAGTCTGAC CTTTATTTGGGTTCCCGTTTTGA
cher-prom-ap1-D for	CTATGACTTGTTAAGACAGAC TTGATCCACTGGGGAATATTATTATCGCTCCGAGC
Antibody production	
NdeI-NFil for	AACATATGTGTCCCGATTGGGAGCTGTG
XhoI-NFil rev	AACTCGAGTCCCTCGGTATAGATCTTGAAG
qRT-PCR	
RECK iQ for	GAGGTAATCTTCGGCCGTTTGG
RECK iQ rev	CGCTTTCTATACACCGTCGCAG
mmp1 iQ for	AGGGCGACAAGTACTACAAGCTGA
mmp1 iQ rev	ACGTCTTGCCGTTCTTGTAGGTGA
dia iQ for	GAATTCGGCGGTTAAGAACCTG
dia iQ rev	GCATAGTACTCGCTGAGGTCC
wasp iQ for	GGTTACGCGTCTCTATGGTGG
wasp iQ rev	CAAGAACGAGCTAATCTGGGAG
cher iQ for	ACAAACCCGTGATCCAGGACAA
cher iQ rev	AGGCCGGGTCCGTAGGCAG
sn iQ for	AAGTACATGACCGCGGAGACCTTT
sn iQ rev	CGTTGCCAAACTGATCGACCGAAA
rac iQ for	TGATCAGCTACACGACCAATG
rac iQ rev	AGCGAGAAGCAGATGAGGAAG
rho iQ for	TCTATGTGCCCACCGTATTCG
rho iQ rev	ATCAGTATGACGTCAGTGTCG
chic iQ for	TCTCCAAGTTTCTCTACCACGG
chic iQ rev	CATTTACCTTTCCGGCACAGAC
rp49 iQ for	TCCTACCAGCTTCAAGATGAC
rp49 iQ rev	CACGTTGTGCACCAGGAACT
ru iQ for	CATTATCCTCGCCACGCTCCT
ru iQ rev	CAGGGCATAGCTAAGGAATC
sev iQ for	ACATCCAGCGCACCGGTAGC
sev iQ rev	CTGCAGTTATCTGGAGGACATG
ex IQ for	TCACTAGATTTGCTGCCCAAGG
ex IQ rev	AATCCCAGACCAAGACCCAAGT
dally IQ for	TCTCCTCAAGATGCACTACTGC
dally IQ for	GTTCAGGGAGTCGACTACACC